Springer

Acta Mechanica Sinica

CrossMark click for updates

• RESEARCH PAPER •

Acta Mech. Sin., Vol. 40, 423609 (2024)
https://doi.org/10.1007/s10409-024-23609-x

Snapthrough response of an innovative symmetric bistable composite wing

Sara Hijazi, and Samir Emam*

Department of Mechanical Engineering, American University of Sharjah, Sharjah PO Box 26666, United Arab Emirates

Received January 20, 2024; accepted February 23, 2024; published online June 13, 2024

This study presents a numerical investigation into the equilibrium shapes and snapthrough response of an innovative bistable symmetric composite wing. The proposed design is a compound plate that consists of a symmetric flat platform followed by a winglet that utilizes the modified hybrid bistable symmetric laminate recently developed in the reference. The hybrid layup of the winglet resolves the issue of losing the bistability of the unsymmetric laminate when attached to another structure. An approximate analytical model based on the Rayleigh-Ritz method is developed for the compound plate that considers the geometric nonlinearity, the clamping conditions at the wing root, and the compatibility conditions at the interface. The static equilibrium positions predicted by the model were verified against the ABAQUS finite element (FE) results and an excellent agreement was obtained. The influence of the geometrical and material parameters of the proposed design on the static equilibrium shapes and the snapthrough response was examined. The following parameters were considered: the length ratio of the flat plate to the bistable winglet, the thickness and location of the bidirectional glass epoxy layers, the load location, and the wing's taperness and aspect ratio. All parameters were found significant, and their effects were discussed. The novelty of this work is that it presents the equilibrium shapes and the snapthrough response of a bistable laminate as a part of a bigger compliant structure, which mimics the scenario in real-life applications.

Compound laminate, Bistable wing, Hybrid symmetric laminates, Snapthrough

Citation: S. Hijazi, and S. Emam, Snapthrough response of an innovative symmetric bistable composite wing, Acta Mech. Sin. 40, 423609 (2024), https://doi.org/10.1007/s10409-024-23609-x

1. Introduction

Bistable laminates have been received considerable attention due to their superior properties and potential applications in morphing and energy harvesting [1-5]. A bistable laminate is a composite structure that has two thermally induced natural stable equilibrium positions. In order to snap it from one stable position to the other, a sufficient load must be applied to cross the potential barriers between the two equilibrium positions. Yet, no continuous load is required to maintain the laminate at its new deflected position since it is a self-equilibriated stable position. The bistability of thin unsymmetric laminates of the [0/90] family was first reported by Hyer [6,7], taking into account the geometric nonlinearities within the classical lamination theory. Since then, there has been a continuous research effort on predicting the room-temperature shapes [8-16], identifying the snapthrough-snapback response [17-19], and investigating the influence of the laminate's material and geometrical parameters on the bistability [20]. Analytical, experimental and numerical methods were used [21,22]. A strategy to suppress cross-well vibrations for a bistable square cross-ply laminate using an additional composite strip is studied in Ref. [23]. The study managed to generate a tunable potential energy landscape in a square bistable cross-ply laminate by attaching an additional composite strip. The asymmetry in the energy barrier required to switch between the two equilibrium states of bistable domes is investigated in Ref. [24]. They found that a simple asymmetry indicator could be used to effectively qualify the dome asymmetric bistability, in turn providing simple guidelines for the design of

*Corresponding authors. E-mail addresses: semam@aus.edu (Samir Emam)
Executive Editor: Yan Li

morphing structures with programmable response [24].

Yet, the bistable laminate is assumed to be free at all boundaries, which limits its applications. It was found that the unsymmetric bistable laminates of the [0/90] family lose their bistability when they are attached to another structure or clamped [25]. As such, they cannot be integrated into larger structures. Mattioni et al. [25] were the first to report the issue of the loss of the bistability of unsymmetric laminates when they are clamped. They extended the modelling efforts and proposed a piecewise layup consisting of a symmetric part and an unsymmetric part. Furthermore, the effect of integrating the bistable laminate with a larger compliant structure on the bistability and snapthrough was investigated. The proposed model showed two stable configurations with different curvatures. Another milestone in the development of bistable symmetric laminates was introduced by Li et al. [26]. They developed an analytical model for a hybrid bistable symmetric laminate (HBSL) that consists of a multi-sectioned layup made of aluminum and carbon epoxy prepregs and exhibits two symmetrical equilibrium shapes like the model proposed by Daynes et al. [21]. Nevertheless, the study was restricted to free-free boundary conditions. Mukherjee et al. [27] reported that the HBSL with aluminum plies suffers from mismatching, debonding, and slipping between the metal aluminum plies and the composite prepregs. Therefore, Mukherjee et al. [27] proposed a modified layup where the aluminum plies were replaced by bidirectional (BD) glass epoxy plies that possess thermal expansion coefficients like those of aluminum. The new layup was called modified hybrid bistable symmetric laminate (m-HBSL) [25]. Moreover, the m-HBSL studied in Ref. [27] was clamped at one end and free at the other end. They experimentally tested the proposed design and reported that the issue of slipping and debonding was resolved. They also developed an analytical model for the modified laminate that accounts for the clamped boundary conditions. Recently, Hijazi and Emam [28] studied the effect of the BD plies' thickness, width, and location from the laminate's centerline on the equilibrium shapes and the snapthrough behavior. They modelled the bistable laminate as a clamped bistable plate that possesses symmetric bistable positions.

The use of both upward and downward configurations in a bistable winglet, as shown in Fig. 1, can enhance performance and efficiency benefits, though these advantages may vary depending on application and design. The wing generates more lift as the aircraft accelerates, resulting in stronger wingtip vortices. A vortex creates a drag force that reduces efficiency and increases fuel consumption. The downward winglet is designed to mitigate this effect by redirecting some of the airflow from the wingtip vortices downward. During takeoff and landing, this downward flow

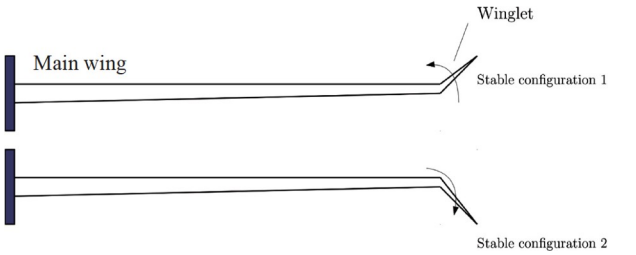

Figure 1 A schematic of the proposed innovative composite wing with upward and downward winglets.

produces a "downwash" that increases the angle of attack of the wing to generate more lift. "Vortex lift" refers to this phenomenon. In certain flight conditions, such as during descent, the downward configuration can also help reduce drag. It can also be helpful to reduce the impact of turbulence on the aircraft during certain turbulent conditions [29]. The upward configuration, on the other hand, can reduce drag and improve stability while cruising. In an upward configuration, the winglet aligns with the airflow, reducing the drag and turbulence created by wingtips. This can result in improved fuel efficiency and range, as well as reduced emissions. The horizontal winglet, on the other hand, is designed to reduce the size of wingtip vortices for drag reduction. Despite this, it does not generate as much lift as the downward winglet since it does not redirect airflow using the vortex lift phenomena. With the horizontal winglet, the pressure is distributed more efficiently across the wing, reducing drag, and improving fuel economy. In summary, the bistable winglet with two positions offers more flexibility than a fixed winglet or a winglet that transitions between vertical and horizontal shapes, as it adapts to a broader range of flight conditions and optimizes wing aerodynamic performance accordingly. An air inlet structure capable of "snapping" open and shut without external force was proposed by Ref. [30], and no external force is required to maintain stable shapes. Further studies by Ref. [31] investigated bistable composite plate activation energy thresholds in order to tailor a bistable system to specific aeronautical applications.

The objective of this paper is to propose an innovative design for a bistable composite wing consisting of a symmetric flat laminate and a symmetrically bistable winglet. The bistability gets induced in the laminate via a thermal curing cycle. The proposed model results in two equilibrium shapes with similar curvatures, unlike the results of the compound plate seen in the model of Mattioni et al. [25]. A bidirectional glass epoxy layer is used in the layup of the winglet to maintain the bistability even when it is attached to the flat planform of the wing and resolve the slipping and debonding issues if aluminum was used instead. A parametric study is excuted to assess the influence of the geometrical and material characteristics on the stable shapes

and the load-deflection response. In particular, the effect of the length ratio of the flat laminate to the bistable laminate is examined. The study also examines the effect of two bi-directional layers' parameters: the thickness and their location from the laminate's centerline across the thickness. Another important factor considered in this study is the location of the applied load, which results in intermediate stable shapes that can be exploited in morphing applications. Finally, the wing's aspect ratio and taperness significance was assessed. The design proposed in this study is provided for the first time in the reference. The novelty of this work is that it presents the snapthrough response of a practical bistable laminate that is part of a bigger structure, which mimics real-life applications. The previous studies were concerned with bistable laminates that are rigidly clamped. The influence of the structural compliance to which the bistable laminate is attached was not studied. For instance, in aerospace and other engineering applications, the bistable panel would be attached to a bigger compliant structure. Therefore, in this work, we considered the existence of a flat symmetric structure that represents the host structure attached to a bistable laminate and analyzed the equilibrium shapes and the snapthrough response of the whole structure. The rest of the paper is as follows: Sect. 2 presents an approximate analytical model for the proposed structure that consists of a flat panel attached with a bistable laminate, Sect. 3 presents a finite element implementation using ABAQUS 2022 learning edition version package and model validation, Sect. 4 presents the results and discussion for the snapthrough response and the effect of various parameters, and Sect. 5 presents some conclusion.

2. Model

The most important feature of using bistable composites compared with other smart structures is that the load to cause change is only required momentarily to initiate the transition. No continuous power is required to keep the structure at one of its self-equilibrated stable positions. In this paper, the analytical model of Mattioni et al. [25] is modified by replacing the unsymmetric plate, the bistable element, with the m-HBSL proposed by Mukherjee et al. [27] and extended by Hijazi and Emam [28]. The proposed model represents a more realistic wing structure that has a clamped flat panel and a symmetrically bistable winglet. A schematic of the proposed design and layup are shown in Figs. 2 and 3. The main wing is made up of the symmetric laminate and the winglet is made up of the m-HBSL. The proposed design is called: innovative hybrid bistable symmetric laminate (i-HBSL). The hybrid layup of the winglet preserves the bistability even when it is attached to the complaint structure of the main wing. A mathematical

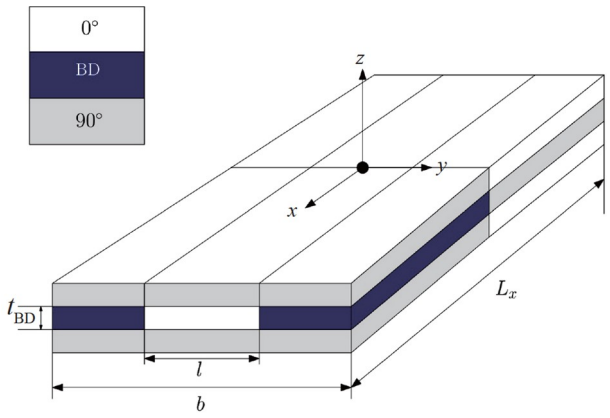

Figure 2 A schematic of the layup of the proposed innovative bistable composite wing.

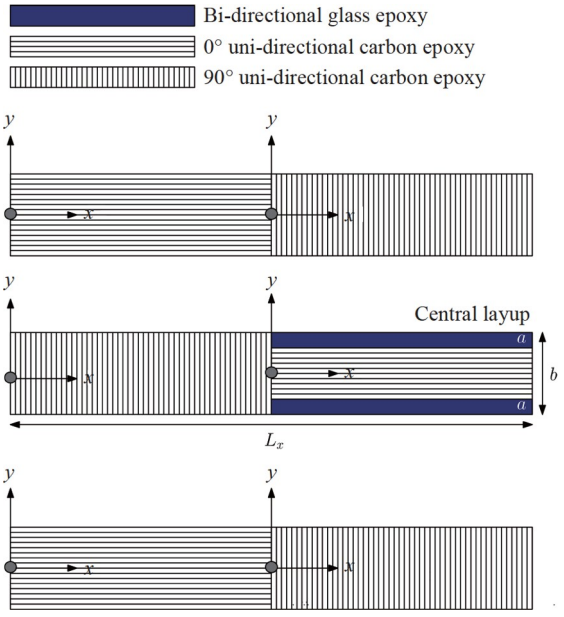

Figure 3 A schematic of the stacking sequence of the proposed i-HBSL.

model is developed to investigate the static configurations and the snapthrough response of the proposed design using the Rayleigh-Ritz method. The wing has a span length of 600 mm and a chord length of 100 mm. The flat plate has a symmetric six-layer stacking sequence of $[0_2/90]_S$ and the bistable plate consists of three sections: two outer sections with the layup $[90_2/\mathrm{BD}_2/90_2]_T$ and an inner section with the layup $[90_2/0_2/90_2]_T$. The flat and bistable segments attached together make the innovative suggested wing structure. It is worth noting that the current study only considers cross-ply laminates that assume cylindrical equilibrium shapes at room temperature. Rotating some layers in the *x*-*y* plane, as shown in Fig. 2, to end up with an angle-ply laminate, will result in warped shapes that cannot be approximated by the current analytical model.

The geometrical parameters that will be examined are the

ratio of the length of the bistable panel to the flat panel and the width, thickness, the location of the bidirectional layers, and the wing's taperness and aspect ratio. The results show that these parameters affect the static equilibrium shapes and the snapthrough response. The material properties of the constituent layers used in this analysis are given in Table 1.

To the mathematical model, we consider a composite wing that consists of a flat plate followed by a bistable plate, as shown in Fig. 4. Let A be the domain of the whole structure such that

$$A = A_1 \cup A_2 , \tag{1}$$

where A_1 represents the domain of the flat plate and A_2 represents the domain of the multi-sectioned bistable plate. Despite the use of a multi-sectioned layup, continuous displacement and strain fields are achieved by assuming piecewise displacement and strain fields and enforcing continuity conditions at the interface. This, however, increases the computational cost due to the increased number of unknowns. The inplane strains at the structure's midplane are assumed as follows [25]:

$$\varepsilon_x^{0(i)} = c_1^{(i)} + c_2^{(i)}x^2 + c_3^{(i)}xy + c_4^{(i)}y^2, \tag{2}$$

$$\varepsilon_y^{0(i)} = c_5^{(i)} + c_6^{(i)}x^2 + c_7^{(i)}xy + c_8^{(i)}y^2. \tag{3}$$

The out-of-plane displacement of the midplane for each plate is assumed in the following form [23]:

$$\begin{aligned} w^{0(i)} = {} & c_9^{(i)} + c_{10}^{(i)}x + c_{11}^{(i)}y + c_{12}^{(i)}x^2 + c_{13}^{(i)}y^2 \\ & + c_{14}^{(i)}xy + c_{15}^{(i)}xy^2 + c_{16}^{(i)}x^2y + c_{17}^{(i)}x^2y^2. \end{aligned} \tag{4}$$

The superscript (i) is set equal to 1 and 2 to represent the first and second plates, respectively. The inplane strains considering von Karman's geometric nonlinearity are defined as [28]:

$$\varepsilon_x^{0(i)} = \frac{\partial u^{0(i)}}{\partial x} + \frac{1}{2}\left(\frac{\partial w^{0(i)}}{\partial x}\right)^2, \tag{5}$$

$$\varepsilon_y^{0(i)} = \frac{\partial v^{0(i)}}{\partial y} + \frac{1}{2}\left(\frac{\partial w^{0(i)}}{\partial y}\right)^2, \tag{6}$$

$$\gamma_{xy}^{0(i)} = \frac{\partial u^{0(i)}}{\partial y} + \frac{\partial v^{0(i)}}{\partial x} + \frac{\partial w^{0(i)}}{\partial x}\frac{\partial w^{0(i)}}{\partial y}. \tag{7}$$

Integrating Eqs. (5) and (6) and solving for the inplane displacements yield

$$u^{0(i)} = \int\left[\varepsilon_x^{0(i)} - \frac{1}{2}\left(\frac{\partial w^{0(i)}}{\partial x}\right)^2\right]\mathrm{d}x + c_{18}^{(i)}y + c_{19}^{(i)}y^3, \tag{8}$$

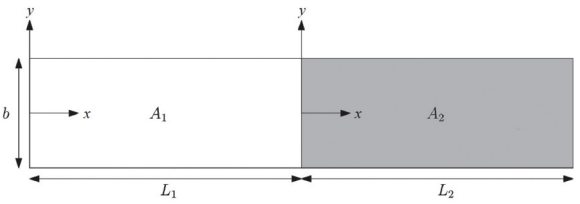

Figure 4 A schematic of the proposed bistable composite wing.

$$v^{0(i)} = \int\left[\varepsilon_y^{0(i)} - \frac{1}{2}\left(\frac{\partial w^{0(i)}}{\partial y}\right)^2\right]\mathrm{d}y + c_{20}^{(i)}x + c_{21}^{(i)}x^3, \tag{9}$$

The midplane strain and curvature vectors $\epsilon^{0(i)}$ and $\boldsymbol{\kappa}^{0(i)}$ are, respectively, defined as:

$$\epsilon^{0(i)} = \begin{Bmatrix} \varepsilon_x^0 \\ \varepsilon_y^0 \\ \gamma_{xy}^0 \end{Bmatrix}^{(i)}, \tag{10}$$

$$\boldsymbol{\kappa}^{0(i)} = \begin{Bmatrix} -\dfrac{\partial^2 w^0}{\partial x^2} \\ -\dfrac{\partial^2 w^0}{\partial y^2} \\ -2\dfrac{\partial^2 w^0}{\partial x \partial y} \end{Bmatrix}^{(i)}. \tag{11}$$

The strain energy of the entire structure can now be calculated by combining the strain energy for each plate taking into consideration their stacking sequences and integration limits. The result is [28]

$$\begin{aligned} \Pi = {} & \frac{1}{2}\iint_{A_1}\left(\begin{bmatrix}\epsilon^{0(1)} \\ \boldsymbol{\kappa}^{0(1)}\end{bmatrix}^{\mathrm{T}}\begin{bmatrix}A^{(1)} & B^{(1)} \\ B^{(1)} & D^{(1)}\end{bmatrix}\begin{bmatrix}\epsilon^{0(1)} \\ \boldsymbol{\kappa}^{0(1)}\end{bmatrix} - \begin{bmatrix}\epsilon^{0(1)} \\ \boldsymbol{\kappa}^{0(1)}\end{bmatrix}^{\mathrm{T}}\begin{bmatrix}N^{\mathrm{th}} \\ M^{\mathrm{th}}\end{bmatrix}^{(1)}\right)\mathrm{d}x\mathrm{d}y \\ & + \frac{1}{2}\iint_{A_2}\left(\begin{bmatrix}\epsilon^{0(2)} \\ \boldsymbol{\kappa}^{0(2)}\end{bmatrix}^{\mathrm{T}}\begin{bmatrix}A^{(2)} & B^{(2)} \\ B^{(2)} & D^{(2)}\end{bmatrix}\begin{bmatrix}\epsilon^{0(2)} \\ \boldsymbol{\kappa}^{0(2)}\end{bmatrix} - \begin{bmatrix}\epsilon^{0(2)} \\ \boldsymbol{\kappa}^{0(2)}\end{bmatrix}^{\mathrm{T}}\begin{bmatrix}N^{\mathrm{th}} \\ M^{\mathrm{th}}\end{bmatrix}^{(2)}\right)\mathrm{d}x\mathrm{d}y, \end{aligned} \tag{12}$$

where $A^{(i)}$, $B^{(i)}$, and $D^{(i)}$ are the laminate's standard extensional, coupling, and bending stiffness matrices, respectively, of the i^{th} plate; $N^{\mathrm{th}\,(i)}$ and $M^{\mathrm{th}\,(i)}$ are the thermally induced force and moment stress resultants, respectively, of the i^{th} plate.

The total strain energy $\Pi = \Pi\left(\mathrm{c}_j^{(i)}\right)$ defined by Eq. (12) is now a function of 42 unknown coefficients for $j = 1, 2, \cdots, 21$, and $i = 1, 2$. The local minima of the total strain energy correspond to the stable equilibrium positions

Table 1 Material properties of carbon epoxy and the bidirectional glass epoxy prepregs used in the analysis [26,27]

Material	E_1 (GPa)	E_2 (GPa)	G_{12} (GPa)	ν_{12}	α_1 (10^{-6}/°C)	α_2 (10^{-6}/°C)	Thickness (mm)
UD carbon epoxy prepreg	137.4	10.07	4.4	0.23	0.37	24.91	0.125
BD glass epoxy prepreg	22.3	22.3	4.75	0.20	19.78	19.78	0.125

of the plate. In order to ensure the continuity of the displacements across the wing domain, the following compatibility conditions must hold [32]:

$$w^{0(1)}(L_1,y) = w^{0(2)}(0,y), \tag{13}$$

$$\frac{\partial w^{0(1)}}{\partial x}(L_1,y) = \frac{\partial w^{0(2)}}{\partial x}(0,y), \tag{14}$$

$$u^{0(1)}(L_1,y) = u^{0(2)}(0,y), \tag{15}$$

$$v^{0(1)}(L_1,y) = v^{0(2)}(0,y). \tag{16}$$

To simplify the equations and computational time, the following assumptions are made [23]:

(1) $c_9^{(1)} = 0$ to satisfy the clamping boundary conditions at the root of the flat plate.

(2) The experimental results showed that the stable configurations are symmetric with respect to x-axis for $i = 1,2$, [25,27]. Therefore the following terms can be elimnated: $c_{11}^{(i)}$, $c_{14}^{(i)}$, $c_{16}^{(i)}$.

(3) The drilling degree of freedom is eliminated for both plates, i.e., $c_{18}^{(i)} = c_{20}^{(i)}$ [25,27].

A non-linear constrained optimization method in MATLAB has been used to find the minima of $\Pi = \Pi\left(c_j^{(i)}\right)$ subject to the constraints defined by Eqs. (13)-(16) to find the stable equilibrium positions of the wing. The analysis has been carried out using the commercial optimization package "mincing" in MATLAB and the required constraints were set as nonlinear constraints for the optimization tool.

Before we delve into the results of the snapthrough response, it is helpful to shed light on the mechanics behind the bistable system in terms of the potential energy landscape. A multistable system can transition from one state of minimal energy to another if given enough external activation energy to overcome the barrier between the stable states, as given in Fig. 5 [33]. This feature reflects the highly nonlinear character of bistable systems.

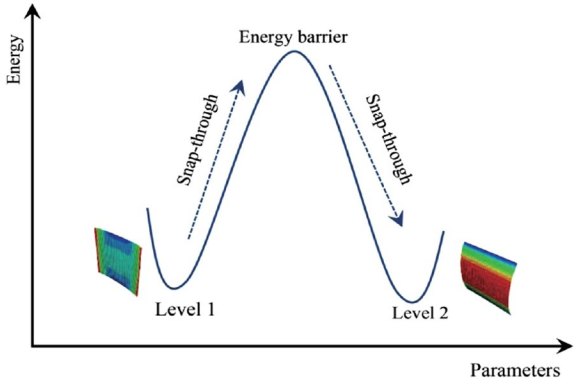

Figure 5 Potential energy landscape of bistable configurations [33].

3. Finite element implementation and model validation

The equilibrium shapes and snapthrough/snapback response of the proposed design are obtained in ABAQUS® finite element (FE) package using the "Static, Stabilize Procedure". The wing structure is modelled using the four-node shell elements (S4R). The option Neom is kept on during the analysis to account for the geometric nonlinearity. To ensure convergence and accuracy of the results, an artificial damping factor is introduced. The equilibrium shapes with clamped boundary conditions are obtained using two steps.

In the first step, an initial uniform temperature field of 150° is applied over the entire model. The laminate is then cooled to room temperature at 30° and an unstable flat configuration is obtained during this step due to the symmetry in the layup. In the second step, the clamped boundary conditions are added on the appropriate locations and a nonzero concentrated point load is applied at the center of the free edge in the transversal direction. Subsequently, the applied load is removed using an empty step and the laminate settles to one of the two stable equilibrium shapes. To obtain the second equilibrium stable shape, the direction of the concentrated load is reversed, and the procedure is repeated. A flowchart that shows the steps of the procedure is shown in Fig. 6. For the snapthrough analysis, two additional steps are added in the ABAQUS procedure presented in the previous section.

(1) A concentrated point load is applied at the center of the free edge, in the direction opposite to the applied test load in the previous steps.

(2) The applied load is removed in the final step and the

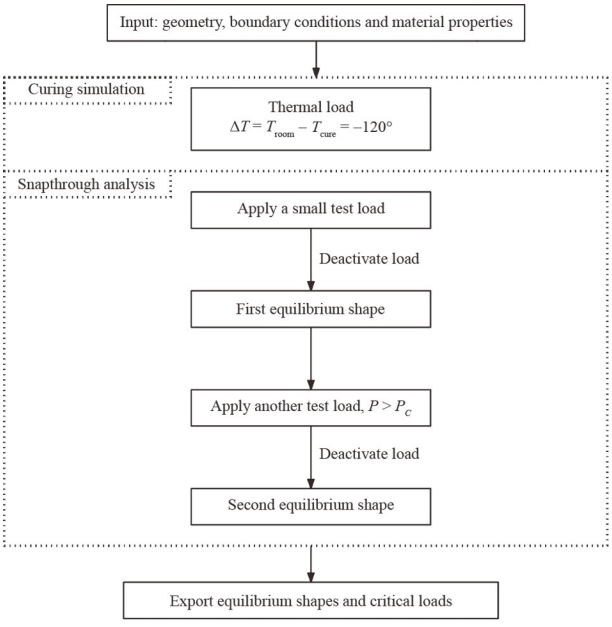

Figure 6 ABAQUS FE simulation flowchart.

model settles to the other equilibrium stable configuration.

It is worth mentioning that 692 elements were used in this study. A mesh sensitivity analysis was performed and the number of elements was kept the least to adequately capture the response in order to reduce the computational time.

3.1 Snapthrough analysis

The snapthrough analysis describes the static response where a lateral load is applied and increased gradually until it reaches a critical value, called the snapthrough load, at which the structure experiences a large-amplitude displacement and jumps to the other stable position. As the load is increased further, the structure monotonically deforms. If the load direction is reversed and the process is repeated, one obtains the snapback load and the load-deflection curves for the loading and unloading are produced. This section presents the load-deflection curves for the proposed wing structure and the snapthrough/snapback loads for a variety of parameters.

3.2 Model validation

For validation purposes, the equilibrium shapes obtained using the current analytical model are validated against the experimental and ABAQUS FE results of Ref. [25]. The 360-mm long structure consists of a symmetric square 4-ply laminate $[0/90]_S$ that is attached to an unsymmetric square 4-ply laminate $[90_2/0_2]_T$. The material properties of the laminate proposed by Mattioni et al. [25] are shown in Table 2. An excellent agreement between the results of the currnet model and the experimental and ABAQUS FE results of Ref. [25] is obtained, as shown in Fig. 7. Figure 8 shows the two stable equilibrium positions obtained using the ABAQUS FE. It is apparent that the unsymmetric plate, basically the bistable structure, loses its bistability when it is attached to the flat symmetric plate, as reported by Mattioni et al. [25]. To validate the analytical model against the snapthrough analysis, we present the snapthrough load predicted by the analytical model and compare it with the peer results obtained using ABAQUS FE analysis. The

Table 2 Material properties of the compound plate [25] used for the model validation

E_1 (GPa)	E_2 (GPa)	G_{12} (GPa)	ν_{12}	α_1 (10^{-6}/°C)	α_2 (10^{-6}/°C)	t_{ply} (mm)
130	10	4.4	0.33	−0.18	30	0.125

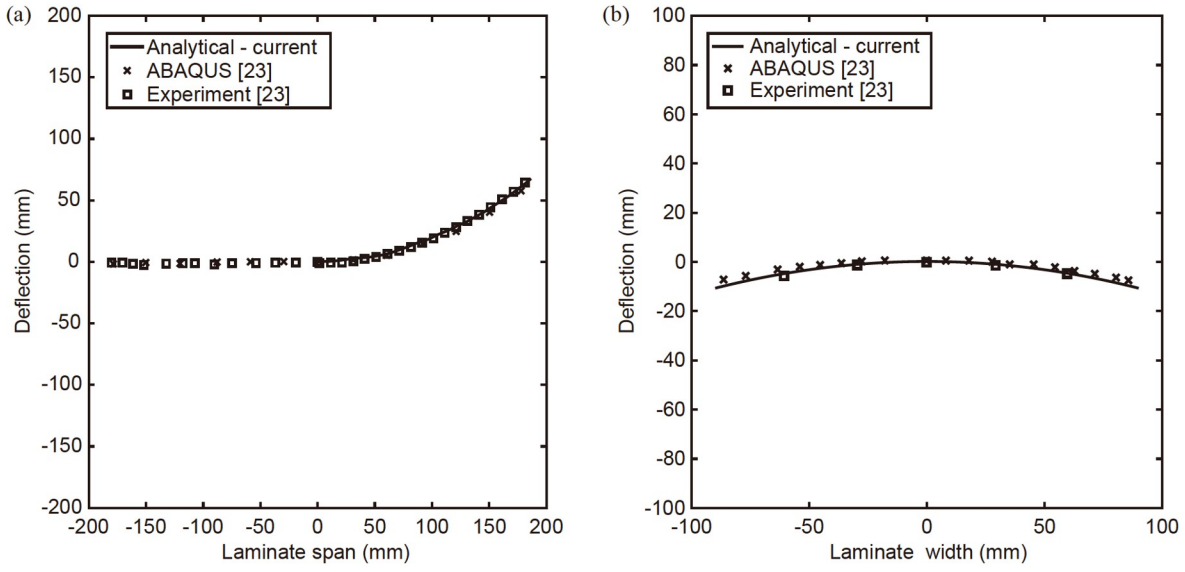

Figure 7 A comparison of the results of the current model and the ABAQUS FE and the experimental results of Ref. [23]. (a) Longitudinal cross section of the curled configuration, (b) unsymmetric cross section of the flat configuration.

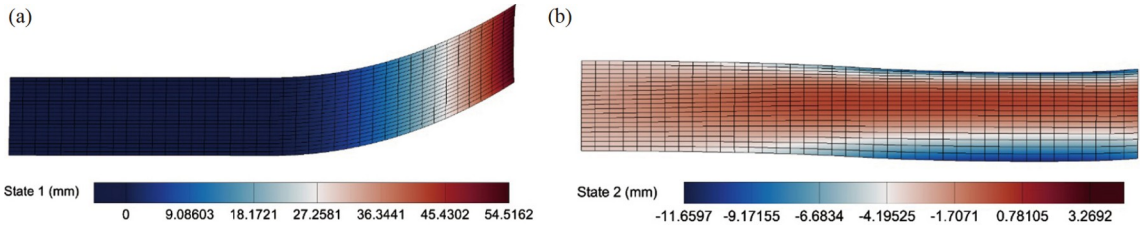

Figure 8 Stable equilibrium shapes of the compound plate obtained using ABAQUS FE. (a) Curled configuration, (b) flat configuration.

comparison is applied on a 300-mm long, 100-mm wide cantilevered m-HBS laminate with the following layup $[90_2/BD_2/90_2]_T \cup [90_2/0_2/90_2]_T \cup [90_2/BD_2/90_2]_T$ whose material properties are given in Table 2. A comparison of the snapthrough loads using the analytical model and ABAQUS FE is given in Table 3, which $2a$ denotes the width of the BD layers and b denotes the total width.

In the present work, we extend the work of Ref. [25] by replacing the unsymmetric laminate with a hybrid symmetric laminate that is able to keep its bistability even when it is attached to another compliant structure. The equilibrium shapes of the compound plate are named "flat configuration" and "curled configuration" and hence the curvature values of the two shapes are not the same.

4. Results and discussion

In this section, the results obtained using the current analytical model for the stable equilibrium positions of the proposed wing are presented. A parametric study that aims at investigating the effect of attaching a multi-sectioned symmetric laminate to a larger structure on the bistability behavior is presented. The parametric study also investigates the effect of the load position, length of the symmetric plate on the snapthrough behavior, and the wing's taperness and aspect ratio. The analysis is based on a fixed BD layer width of 50 mm, i.e., $2a/b = 0.5$.

For the baseline configuration, the symmetric flat and multi-sectioned bistable plates are assumed of the same length, i.e., $L_1/L_2 = 1$. The equilibrium shapes of the proposed innovative composite wing are shown in Fig. 9 using ABAQUS FE. As the figure shows, the wing structure exhibits two symmetric stable positions and the issue of losing the bistability when attaching the bistable plate to another structure is resolved. This shows the ability of the hybrid symmetric laminate to overcome the loss of bistability that the conventional unsymmetric laminates suffered from. It also opens the horizon for the bistable laminates as potential candidates in morphing applications. A comparison between the stable shapes using the analytical model and the ABAQUS FE is shown in Fig. 10 and an excellent agreement is achieved.

A bistable laminate's snapthrough properties change significantly when the laminate is clamped. The reference has many studies that are concerned with the stable shapes and snapthrough response of bistable laminates. Nevertheless, most of these studies are limited to the free-free boundary conditions. When deploying bistable laminates for structural applications, it is extremely important to understand the nonlinear snapthrough phenomenon. This is achieved by analyzing the snapthrough of the i-HBSL proposed model under various loading conditions and geometrical parameters. Yet, the flat plate and the bistable plate are of the same length, 300 mm each. Next, we present the influence of the length ratio, L_1/L_2, the bidirectional BD thickness and location across the thickness, the point of application of the load, the wing's taperness and aspect ratio on the stable equilibrium position and the snapthrough/snapback response.

4.1 Effect of the length ratio L_1/L_2 on the static behavior

The first parameter to consider is the length ratio of the flat plate L_1 to the bistable plate L_2, as shown in Fig. 11. The equilibrium shapes and the load-deflection curves are obtained with varying length ratios L_1/L_2 while all other geometrical and material parameters are kept unchanged.

Figure 12(a) presents the two stable positions of the proposed wing for a length ratio of 1 and 2, respectively. The bidirectional layer width to the overall width is $2a/b =$

Table 3 A comparison of the snapthrough loads of a cantilevered m-HBSL using the analytical and ABAQUS FE models

Bidirectional layers dimensions		Snapthrough load (N)		
Width (mm)	Thickness (mm)	Analytical model	ABAQUS FE model	% Error
40	0.250	0.530	0.526	0.755
50		0.675	0.682	1.037
50	0.500	1.180	1.202	1.864

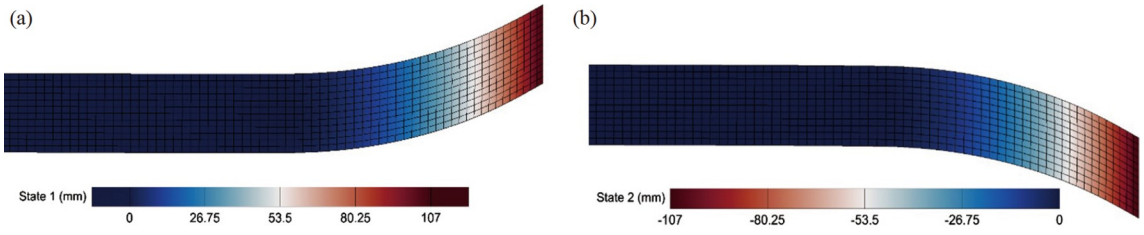

Figure 9 Stable equilibrium shapes of the innovative composite wing. (a) First stable position, (b) second stable position.

0.5 in both cases. As Fig. 12(a) shows, it is observed that changing the length of the flat plate L_1 does not influence the curvature of the equilibrium shapes. This can be interpreted as the bistable plate is clamped with the flat plate in both cases and the curvature of the stable positions depends on the parameters of the bistable plate. On the other hand, the load-deflection curves for the loading and unloading schemes show the significance of the length ratio, as shown in Fig. 12(b). It is seen that as the length of the flat plate increases, the stiffness of the structure decreases evidenced by the reduced slope, which results in more deflection up to the snapthrough event. It can also be noticed that in both cases, the structure's tip deflection at zero load is unchanged. As the figure implies, the blue curve, where the flat panel become twice the bistable panel, the structure deflects more under the same amount of load. Meanwhile, the jump from one equilibrium position to another occurs at the same load. The snapthrough load and the snapback load were found to be insensitive to the length ratio L_1/L_2. The snapthrough load was found to be 0.570 and 0.512 N for a length ratio of 1 and 2, respectively.

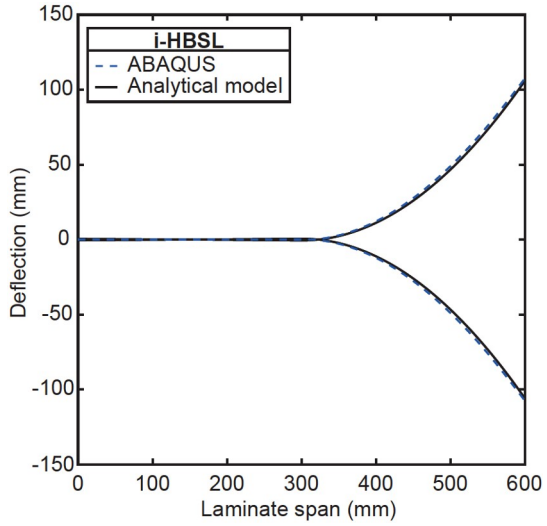

Figure 10 Bistable shapes of the innovative composite wing (i-HBSL) using the analytical.

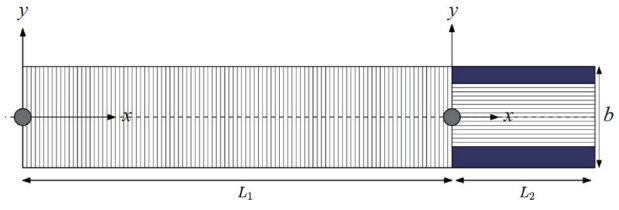

Figure 11 A schematic of the proposed innovative bistable composite wing with varying L_1.

4.2 Effect of the BD glass epoxy layer thickness

The effect of the BD glass epoxy layer thickness is discussed in this section. It is observed that changing the thickness of the BD layers, at the expense of the thickness of the 90° plies, has a significant impact on the snapthrough loads and the equilibrium shapes. The baseline laminate is a six-layer layup that consists of two $[90_2/\mathrm{BD}_2/90_2]$ in the outer sides and $[90_2/0_2/90_2]$ in the core. Each ply is 0.125 mm thick. This means that the thickness of the BD layers of the baseline structure is 0.25 mm (2 plies). In this section, the BD thickness t^*_{BD} is increased to 0.50 and 0.75 mm, which corresponds to the outer side layup of $[90/\mathrm{BD}_4/90]$ and $[\mathrm{BD}_6]$, respectively. The latter layup where t^*_{BD} =0.75 mm, the outer segments of the laminate are made

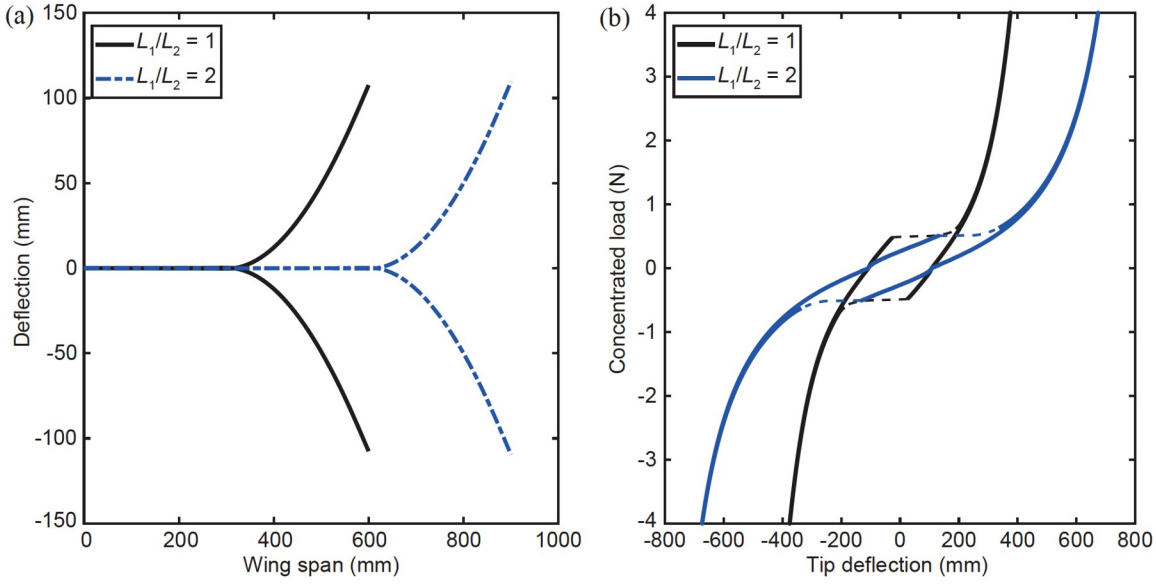

Figure 12 (a) Stable equilibrium shapes, (b) load-deflection curves for various L_1/L_2 ratios.

entirely of the BD plies. Therefore, the total thickness of the flat and bistable parts remains unchanged at 0.75 mm in all cases. It is found that increasing the thickness of the bidirectional glass epoxy layers increases the snapthrough loads and decreases the tip deflection of the laminate. Figure 13 shows the equilibrium shapes and the load-deflection curves obtained for three different values of the BD layer's thickness. The tip deflection decreases as the BD layer's thickness increases, as shown in Fig. 13(a). On the other hand, the load-deflection curves in Fig. 13(b) show that as the thickness of the bi-directional layer t_{BD} increases, the laminate's stiffness increases, and hence the snapthrough load increases. Quantitatively, the tip deflection was reduced by more than 50% upon increasing the BD thickness three times, as shown in Fig. 13(a).

Figure 14 shows the contour maps of the longitudinal curvatures κ_x for various values of the BD layer thickness. Comparing the longitudinal curvature contour distribution for the baseline configuration where $t_{BD} =$ 0.25 mm to the case where $t^*_{BD} =$ 0.75 mm, a change in the curvature κ_x is seen at the interface between the flat plate and the bistable plate. Therefore, the flat plate experiences a change in the curvature when the BD layer thickness is increased beyond a certain ratio, which indicates that the effect of the bidirectional layers is now extended to the flat plate, causing a curvature along the x-axis.

4.3 Effect of the BD glass epoxy layer location across the thickness

This subsection examines the influence of the location of the bidirectional glass epoxy layer with respect to the middle plane on the equilibrium shapes and load-deflection curves of the i-HBSL. The parameter z_{BD}/h indicates the position of the bidirectional glass epoxy measured from the middle plane. When z_{BD}/h is set to 0, the bidirectional glass epoxy layers are positioned at the midplane of the laminate, as illustrated in Fig. 15(a). When z_{BD}/h is set to ±0.5, the bidirectional glass epoxy layers are placed one layer above and below the laminate midplane, as shown in Fig. 15(b). Lastly, when z_{BD}/h is set to ±1, the bidirectional glass epoxy layers are positioned at the top and bottom layers of the laminate, as shown in Fig. 15(c).

Relocating the bidirectional glass epoxy layers has a significant impact on the equilibrium shapes, snapthrough response, and longitudinal curvature distribution. Figure 16(a)

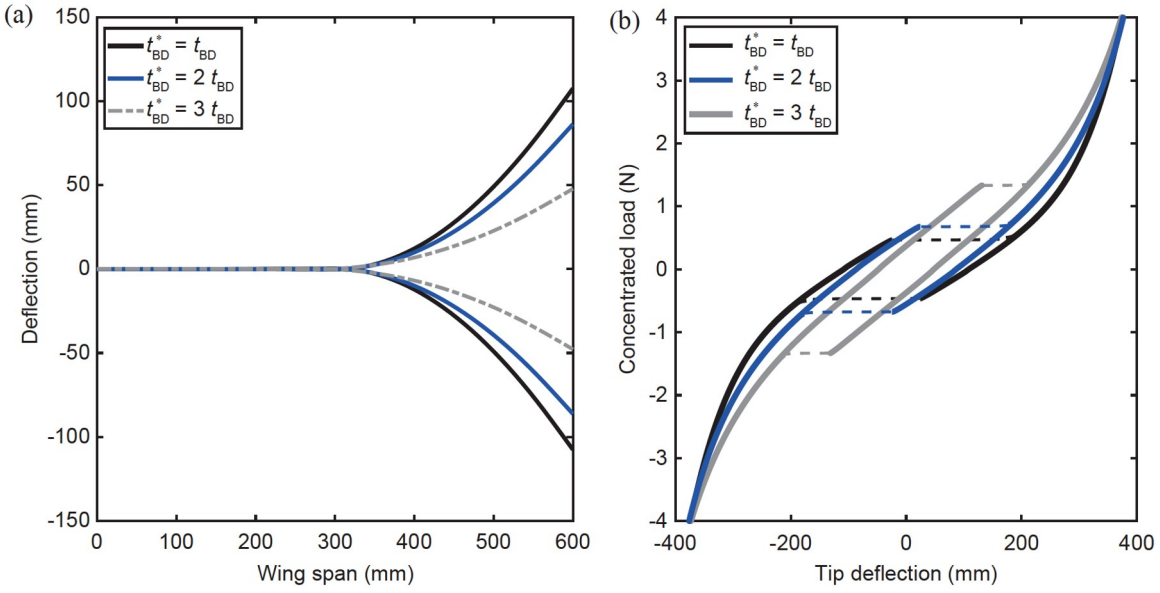

Figure 13 (a) The stable equilibrium shapes, (b) load-deflection curves with varying bidirectional plies' thickness.

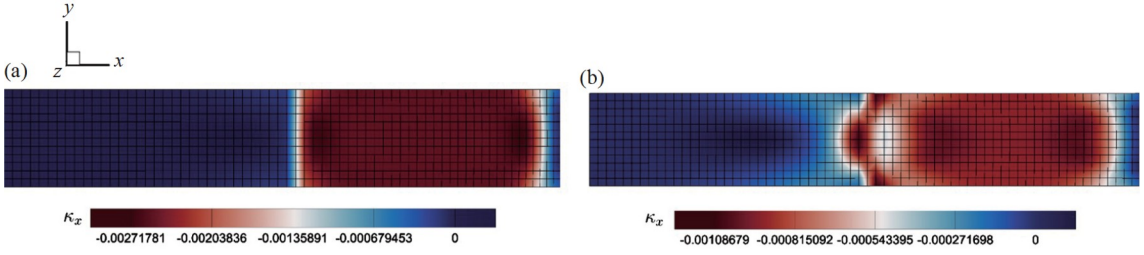

Figure 14 Contour maps of the longitudinal curvature κ_x at different BD layer thickness. (a) t_{BD} = 0.25 mm, (b) t_{BD} = 0.75 mm.

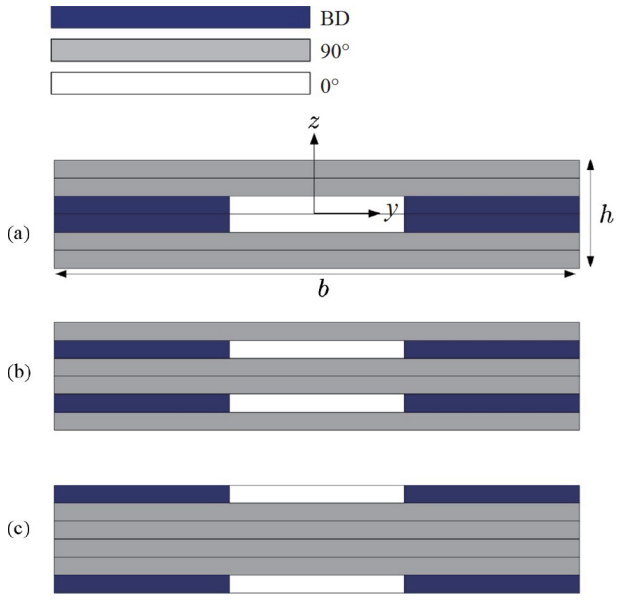

Figure 15 Schematic figure of i-HBSL at different BD location. (a) $z_{BD}/h = 0$, (b) $z_{BD}/h = \pm 0.5$, (c) $z_{BD}/h = \pm 1$.

shows the equilibrium shapes of the i-HBSL for different configurations: $z_{BD}/h = 0$, $z_{BD}/h = 0.5$ and $z_{BD}/h = 1$. The results show that as the BD layers are placed away from the laminate's midplane, the laminate gains stiffness, the tip deflection decreases, and the snapthrough load increases. Namely, when the BD layers are moved from the laminate's centerline to its edges, i.e., from $z_{BD}/h = 0$ to $z_{BD}/h = \pm 1$, the tip deflection is reduced by 46% and the snapthrough load is increased by around 41%. Therefore, the location of the bidirectional layers has a key role in the laminate's behavior, and hence it is an important design parameter.

The contour maps of midplane strains ϵ_x^0 and ϵ_y^0 are shown in Fig. 16 for the two configurations: $z_{BD}/h = 0$ and $z_{BD}/h = \pm 1$. FEA results show that the midplane strain varies when the location of the bidirectional layers is changed. Figure 17(c) and (d) show the distribution of the midplane strains when the bidirectional layers are placed one layer away from the centerline, and the two 90° composite plies of the hybrid and central region are placed at the midplane of the laminate. The strain distribution values in the x and y directions for $z_{BD}/h = \pm 1$ are lower than the overall strain distribution seen for the baseline configuration at $z_{BD}/h = 0$. In addition, the midplane strain ϵ_x^0 in the central region is assumed to be quadratic in the x-direction and vary linearly along the y-direction in the hybrid region, as seen in Fig. 17(c). Whereas the midplane strain ϵ_y^0 is assumed to be continuous along the ϵ_y^0 and independent of x. This is the opposite of the colormap obtained with the base configuration, i.e., $z_{BD}/h = 0$.

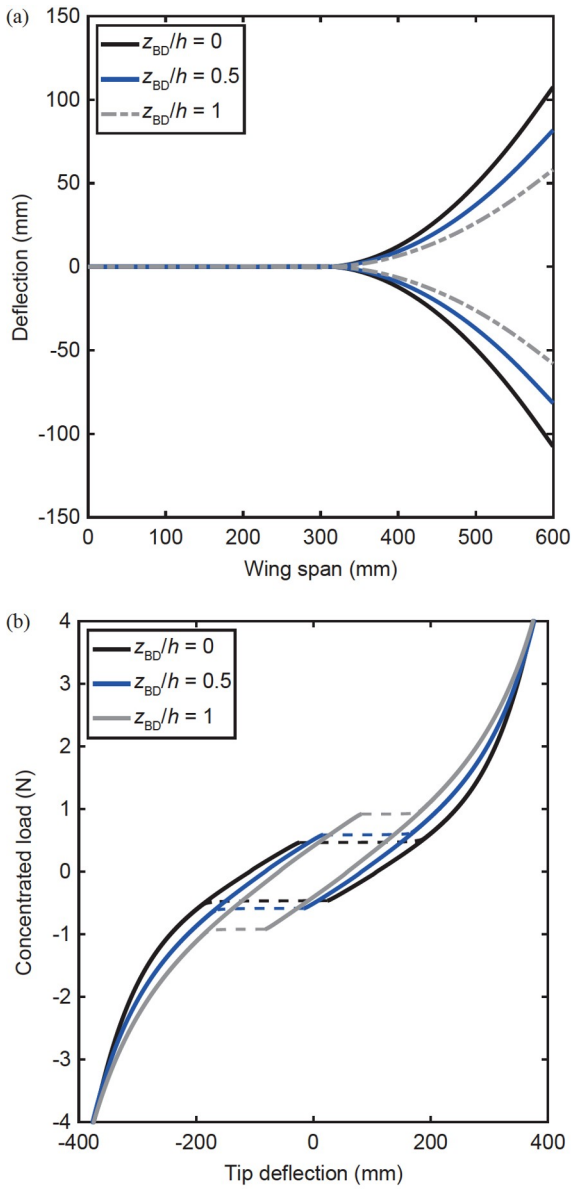

Figure 16 (a) The stable equilibrium shapes of the i-HBSL, (b) load-deflection curves with varying bidirectional plies' location.

4.4 Effect of the concentrated load location

Here, we consider the effect of the point of application of the concentrated load on the deflected shapes and the load-deflection behavior. The load position is varied along the laminate's longitudinal axis, the x-axis, such that $L_p/L_2 = 1$, 0.7, and 0.5 that correspond to the points: P_1, P_2, and P_3, respectively, as shown in Fig. 18. As can be seen from Fig. 18, the location of the applied load is qualitatively and quantitatively significant. The deflected configurations vary with the load location. Moreover, the load-deflection curves show that as the load is moved away from the tip, the snapthrough load increases due to the decrease of the effective length. In addition, it is seen that the two stable

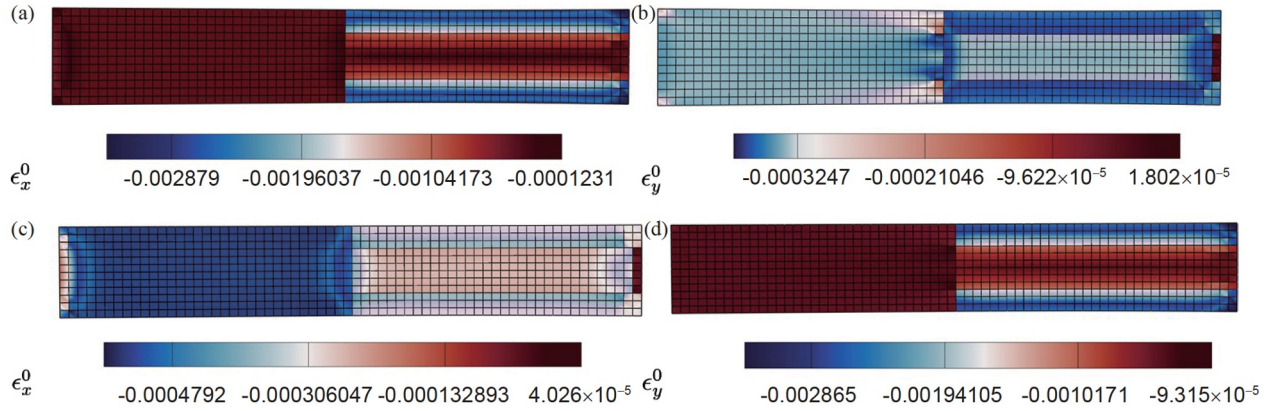

Figure 17 Contour maps of mid-plane strain at different BD layer locations. (a), (b) $z_{BD}/h = 0$, (c), (d) $z_{BD}/h = 1$.

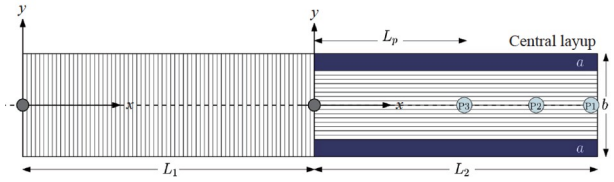

Figure 18 Schematic figure of the applied load at different locations.

shapes lose symmetry when the load is applied near the flat plate although the laminate is symmetric. Figure 19 shows the intermediate stable equilibrium shapes for $L_p/L_2 = 0.5$ and 0.7. The energy loss per loading cycle that is the enclosed area under the loading/unloading plots reduces as the load is moved away from the tip. This can be interpreted as the load is moved away from the tip, the effective length of the structure becomes shorter and hence the energy loss due to loading/unloading decreases. This feature of breaking the symmetry of the deflected shape of a symmetric laminate due to the load location can be utilized in morphing applications, the stable configurations in 3D are shown in Fig. 20.

4.5 Effect of the wing taperness and aspect ratio

Here, we explore the significance of the wing taperness and aspect ratio on the load-deflection and snapthrough/snapback response. The wing is assumed to have a chord length c_r at the root and c_t at the tip, and a mean chord c_m, as shown in Fig. 21. The aspect ratio is defined as the ratio of the wing length L_x to the mean chord length c_m. The taperness ratio c_r/c_t and the aspect ratio L_x/c_m are varied independently and the stable equilibrium shapes and the load-deflection curves are obtained.

The first set of parameters is $L_x = 600$ mm, $c_t = 100$ mm, and c_r is allowed to vary. It is found out that the taperness ratio c_r/c_t has a significant effect on the stable equilibrium shapes and the load-deflection curves. Moreover, the taper ratio of 2, for the set of parameters used, was found to yield the least curvature of the stable shape and highest snap-

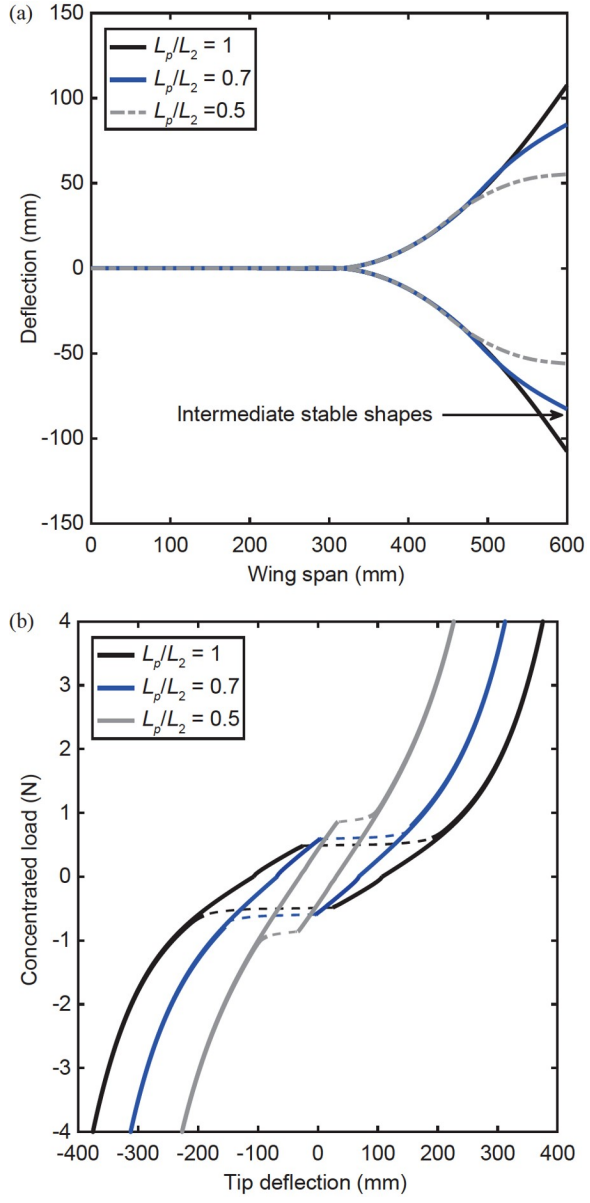

Figure 19 (a) The stable equilibrium shapes, (b) load-deflection curves with varying bidirectional plies' thickness.

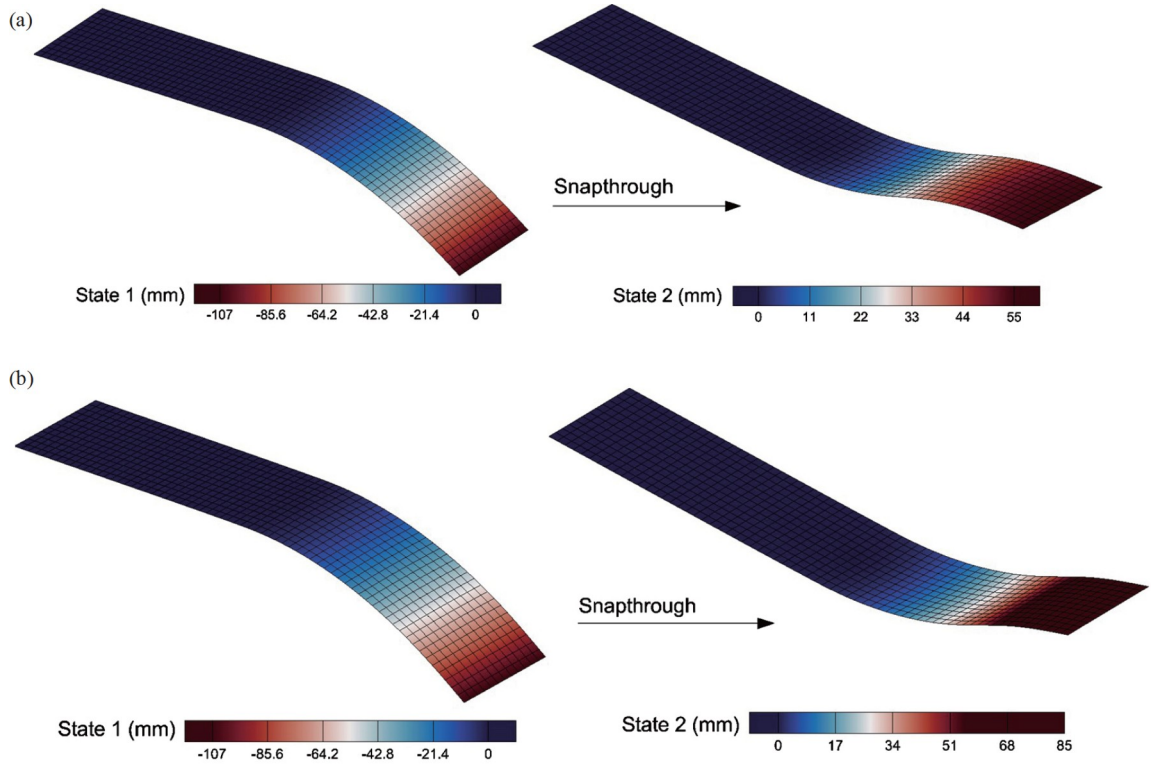

Figure 20 The intermediate shapes at different load locations. (a) $L_p/L_2 = 0.7$, (b) $L_p/L_2 = 0.5$.

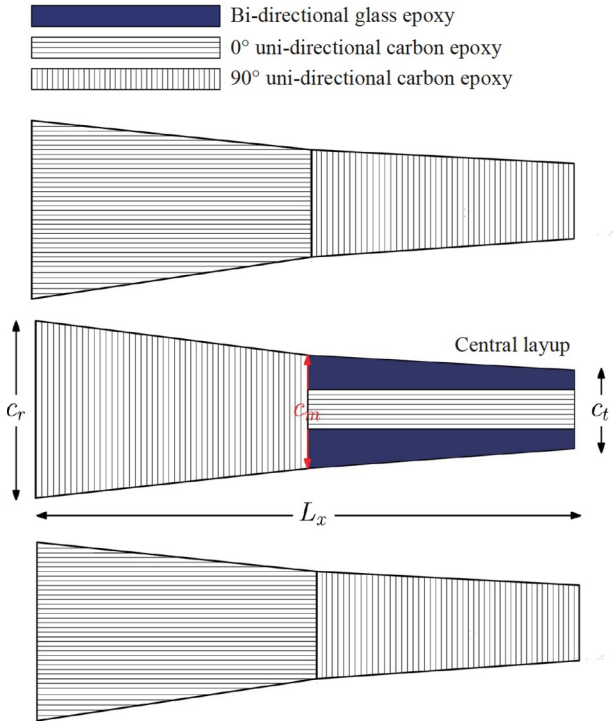

Figure 21 Schematic figure of a straight tapered wing showing the upper, lower, and intermediate layers.

through load, as shown in Fig. 22. The results reveal that there is a threshold for the taperness ratio c_r/c_t beyond which the stiffness of the structure and hence the tip static deflection reverse the trend. In particular, and for the set of parameters used in this study, it was found that the ratio of 2 would result in the maximum stiffness and hence the minimum tip deflection. Beyond this ratio, the stiffness decreases and tip deflection increases. This features a design aspect of tapered bistable laminates. Next, we examine how the aspect ratio impacts the stable equilibrium shape and snapthrough load of a bistable wing. In this analysis, the taper ratio is fixed at $c_r/c_t = 2$. The results demonstrate that as the aspect ratio increases, the snapthrough load decreases, as seen in Fig. 23. Meanwhile, the strain energy stored up to the moment of snapthrough increases as the aspect ratio increases. The variation of the flexibility and energy absorption with the aspect ratio highlights its significance in design against impacts.

5. Conclusion

This study presented a numerical investigation into the room-temperature shapes and snapthrough of a thermally induced bistable innovative wing. The proposed innovative bistable composite wing consists of a symmetric flat platform followed by a winglet that utilizes the modified hybrid symmetric bistable laminate. An approximate analytical model based on the Raleigh-Ritz method is used to find the

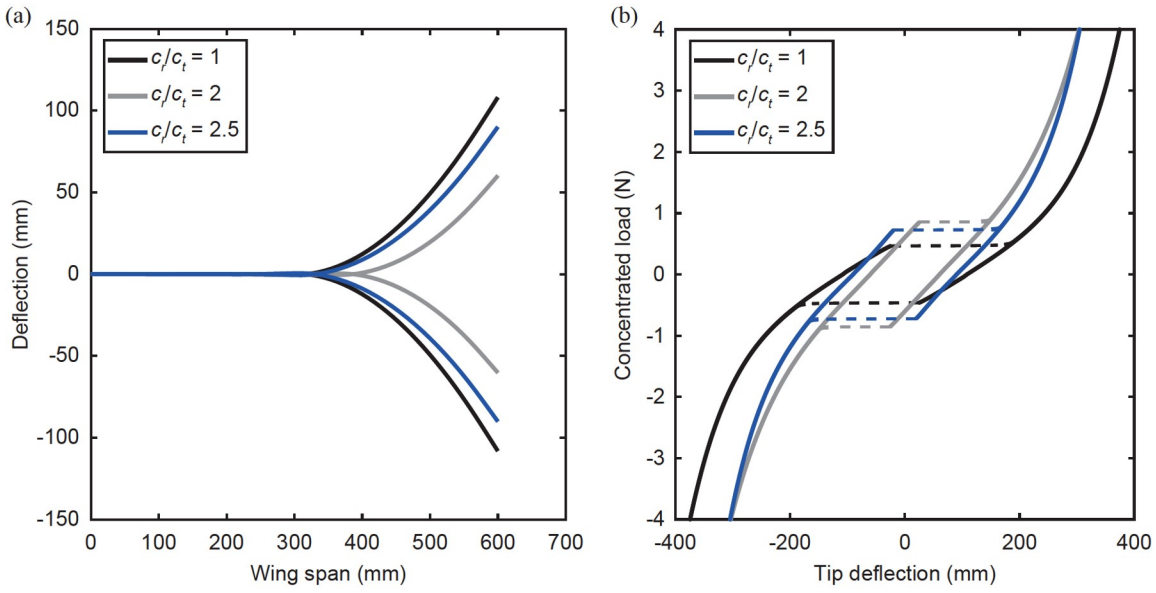

Figure 22 (a) Stable equilibrium shapes, (b) load-deflection curves at different taper ratios c_r/c_t.

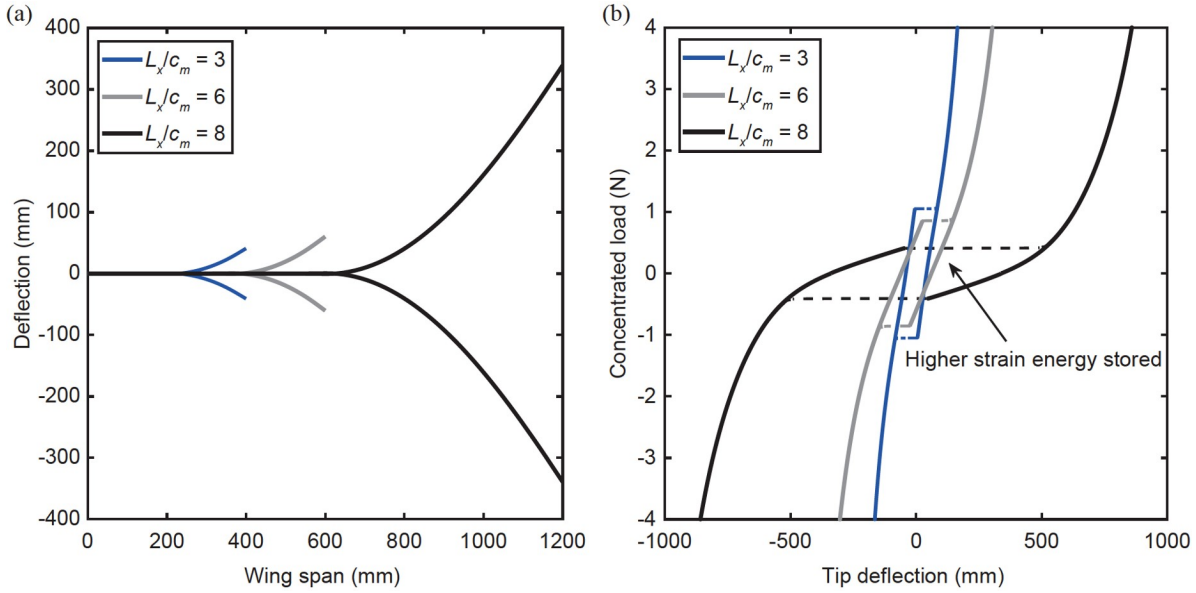

Figure 23 (a) Stable equilibrium shapes, (b) load-deflection curves at varying aspect ratios.

stable equilibrium positions and it showed an excellent agreement compared with the experimental and FE results. The ABAQUS FE package is used to find the load-deflection plots and the snapthrough/snapback loads. A parametric study was performed to examine the influence of the BD layer parameters, the ratio of the flat plate to the bistable plate, the location of the load, and the wing's taperness and aspect ratio on the laminate's response. Two BD parameters were considered: its thickness and location along the wing's cross section. It was found that increasing the thickness of the BD glass epoxy layer increases the stiffness of the wing where the overall thickness of the structure was unchanged. It was found that moving the two BD layers from the laminate's midplane to its bottom and top resulted in a reduction of the tip deflection by 46% and an increase in the snapthrough load by 41%. In terms of the BD thickness effect, it was found that the tip deflection reduces from 107 to 50 mm, about 47% reduction, when the BD thickness increased three times. The flexibility of the structure can also be controlled by varying the length of the symmetric flat platform. Results showed that increasing the length ratio of the flat and bistable plates softens the structure. However, the length ratio showed an insignificant effect on the snapthrough load. For morphing applications, the ability to ob-

tain different stable shapes was found to be greatly affected by the location of the applied concentrated load. Results showed a new set of stable shapes named "intermediate stable shapes" upon changing the location of the applied load. The wing's taperness and aspect ratio were also found to yield different curvatures and stiffnesses. As a future work, the mechanism to trigger the snapthrough remains a challenge and the dynamic response due to time-dependent loads is not available in the reference for clamped bistable laminates. Meanwhile, there is a gap in the reference that experimental results may be performed and compared with the approximate analytical and numerical results presented in this work. Moreover, the behavior of the bistable laminates to dynamic loading is an open area of research.

Conflict of interest *On behalf of all authors, the corresponding author states that there is no conflict of interest.*

Author contributions ***Sara Hijazi:*** *Methodology, first draft of the manuscript, finite element results, project administration.* ***Samir Emam:*** *Research planning, review and organize the manuscript, conceptualization, formal analysis, project administration, resources, validation.*

Acknowledgements *This work was supported by the Project of American University of Sharjah (Grant No. FRG21-M-E92).*

1 S. A. Emam, and D. J. Inman, A review on bistable composite laminates for morphing and energy harvesting, Appl. Mech. Rev. **67**, 060803 (2015).
2 M. Gude, and W. Hufenbach, Design of novel morphing structures based on bistable composites with piezoceramic actuators, Mech. Compos. Mater. **42**, 339 (2006).
3 C. R. Bowen, R. Butler, R. Jervis, H. A. Kim, and A. I. T. Salo, Morphing and shape control using unsymmetrical composites, J. Intell. Mater. Syst. Struct. **18**, 89 (2007).
4 S. Daynes, and P. Weaver, Analysis of unsymmetric CFRP-metal hybrid laminates for use in adaptive structures, Compos. Part A-Appl. Sci. Manuf. **41**, 1712 (2010).
5 C. G. Diaconu, P. M. Weaver, and F. Mattioni, Concepts for morphing airfoil sections using bi-stable laminated composite structures, Thin-Walled Struct. **46**, 689 (2008).
6 M. W. Hyer, Some observations on the cured shape of thin unsymmetric laminates, J. Compos. Mater. **15**, 175 (1981).
7 M. W. Hyer, The room-temperature shapes of four-layer unsymmetric cross-ply laminates, J. Compos. Mater. **16**, 318 (1982).
8 W. J. Jun, and C. S. Hong, Effect of residual shear strain on the cured shape of unsymmetric cross-ply thin laminates, Compos. Sci. Tech. **38**, 55 (1990).
9 M. Schlecht, K. Schulte, and M. W. Hyer, Advanced calculation of the room-temperature shapes of thin unsymmetric composite laminates, Compos. Struct. **32**, 627 (1995).
10 S. R. White, and H. T. Hahn, Process modeling of composite materials: Residual stress development during cure. Part I. Model formulation, J. Compos. Mater. **26**, 2402 (1992).
11 M. L. Dano, and M. W. Hyer, Thermally-induced deformation behavior of unsymmetric laminates, Int. J. Solids Struct. **35**, 2101 (1998).
12 S. Daynes, C. Diaconu, and P. Weaver, Bistable prestressed symmetric laminates, J. Compos. Mater. **44**, 1119 (2010).
13 C. S. Sousa, P. P. Camanho, and A. Suleman, Analysis of multistable variable stiffness composite plates, Compos. Struct. **98**, 34 (2013).
14 A. Haldar, J. Reinoso, E. Jansen, and R. Rolfes, Thermally induced multistable configurations of variable stiffness composite plates: Semi-analytical and finite element investigation, Compos. Struct. **183**, 161 (2018).
15 P. M. Anilkumar, A. Haldar, E. Jansen, B. N. Rao, and R. Rolfes, Design optimization of multistable variable-stiffness laminates, Mech. Adv. Mater. Struct. **26**, 48 (2019).
16 F. Mattioni, P. M. Weaver, K. D. Potter, and M. I. Friswell, Analysis of thermally induced multistable composites, Int. J. Solids Struct. **45**, 657 (2008).
17 M. R. Schultz, M. W. Hyer, R. Brett Williams, W. Keats Wilkie, and D. J. Inman, Snap-through of unsymmetric laminates using piezo-composite actuators, Compos. Sci. Tech. **66**, 2442 (2006).
18 M. L. Dano, and M. W. Hyer, Snap-through of unsymmetric fiber-reinforced composite laminates, Int. J. Solids Struct. **39**, 175 (2002).
19 S. A. Emam, Snapthrough and free vibration of bistable composite laminates using a simplified Rayleigh-Ritz model, Compos. Struct. **206**, 403 (2018).
20 S. A. Emam, T. Pherwani, A. Anil, and A. Muhammed, Parametric study on the influence of material properties and geometry on the thermally induced bistability of composite laminates, Proc. Inst. Mech. Eng. Part C-J. Mech. Eng. Sci. **236**, 4194 (2022).
21 S. Daynes, P. M. Weaver, and K. D. Potter, Aeroelastic study of bistable composite airfoils, J. Aircr. **46**, 2169 (2009).
22 A. Firouzian-Nejad, C. Bowen, S. Mustapha, M. Ghayour, and S. Ziaei-Rad, Bi-stable hybrid composite laminates containing metallic strips: An experimental and numerical investigation, Smart Mater. Struct. **28**, 055030 (2019).
23 B. Danish, P. M. Anilkumar, and B. N. Rao, Suppression of cross-well vibrations of a bistable square cross-ply laminate using an additional composite strip, Int. J. Dynam. Control **11**, 2680 (2023).
24 F. Albertini, M. G. Tarantino, and L. Daniel, Mechanical behavior of embedded bistable dome shell with tunable energy barrier asymmetry, Int. J. Mech. Sci. **263**, 108762 (2024).
25 F. Mattioni, P. M. Weaver, and M. I. Friswell, Multistable composite plates with piecewise variation of lay-up in the planform, Int. J. Solids Struct. **46**, 151 (2009).
26 H. Li, F. Dai, P. M. Weaver, and S. Du, Bistable hybrid symmetric laminates, Compos. Struct. **116**, 782 (2014).
27 A. Mukherjee, M. I. Friswell, S. F. Ali, and A. Arockiarajan, Modeling and design of a class of hybrid bistable symmetric laminates with cantilever boundary configuration, Compos. Struct. **239**, 112019 (2020).
28 S. Hijazi, and S. Emam, An investigation into the static configurations and snapthrough response of clamped hybrid bistable symmetric laminates, Compos. Struct. **312**, 116880 (2023).
29 M. J. M. Penders, and A. M. J. van Oudheusden, Wingtip fences as an alternative to winglets: A study of their aerodynamic effects, J. Aircr. **49**, 1877 (2012).
30 S. Daynes, P. M. Weaver, and J. A. Trevarthen, A morphing composite air inlet with multiple stable shapes, J. Intell. Mater. Syst. Struct. **22**, 961 (2011).
31 F. Nicassio, G. Scarselli, G. Avanzini, and G. Core, in Numerical and experimental study of bistable plates for morphing structures: Proceedings of the SPIE Smart Structures and Materials + Non-destructive Evaluation and Health Monitoring, Portland, 2017.
32 S. Hijazi, A Static and Snapthrough Analysis of an Innovative Bistable Composite Wing, Dissertation for Master's Degree (American University of Sharjah, Sharjah, 2022).
33 B. Danish, P. M. Anilkumar, A. Haldar, and B. N. Rao, Dynamic response of piezoelectrically actuated bistable cross-ply laminates under oscillating impulse voltages, Mech. Adv. Mater. Struct. (2023).

创新型对称双稳态复合材料翼的快速翻转响应研究

Sara Hijazi, Samir Emam

摘要 本文通过数值研究, 探讨了一种创新设计的双稳态对称复合材料翼的平衡形状和快速翻转响应. 该设计是由一个对称的平板和一个带有小翼尖的复合板组成, 后者采用了文献中新近提出的改进型混合双稳态对称层压板. 小翼尖的混合铺层解决了非对称层压板在连接到另一个结构时失去双稳态的问题. 基于Rayleigh-Ritz方法, 为复合板开发了一个考虑几何非线性、翼根处的夹紧条件以及界面处兼容性条件的近似分析模型. 该模型预测的静态平衡位置与ABAQUS有限元结果进行了验证, 取得了非常好的一致性. 研究还考察了所提设计中的几何和材料参数对静态平衡形状和快速翻转响应的影响. 考虑了以下参数: 平板与双稳态小翼尖的长度比、双向玻璃纤维环氧层厚度及其位置、载荷作用位置以及翼展的锥度和展弦比. 研究发现所有这些参数都具有显著影响, 并对其效应进行了讨论. 这项工作的新颖之处在于, 它将双稳态层压板作为更大柔性结构的一部分来呈现其平衡形状和快速翻转响应, 模仿了实际应用中的情景.